Joint Carrier Frequency Offset, Sampling Time Offset and Channel Estimation in Multiuser OFDM/OQAM Systems

Ali Baghaki, Benoit Champagne
Department of Electrical and Computer Engineering, McGill University, 3480 University Street
Montreal, QC, Canada, H3A 0E9
Email: ali.baghaki@mail.mcgill.ca; benoit.champagne@mcgill.ca

***Abstract*—A derivative of orthogonal frequency division multiplexing (OFDM) based on offset quadrature amplitude modulation, OFDM/OQAM, is among the waveform contenders for future wireless networks. Focusing on multiuser scenarios, i.e. uplink of a multiple access system, we propose an improved joint estimation method for carrier frequency offset, sampling time offset and channel impulse response needed for the practical application of OFDM/OQAM. The proposed method offers a pilot-based maximum-likelihood (ML) estimation of the unknown parameters in multiuser OFDM/OQAM systems. Formulation of the estimator is based on the splitting of each received pilot symbol into contributions from surrounding pilot symbols, non-pilot symbols, additive noise and multiuser interference. The proposed estimator is compared with a highly cited previous work of the same focus where the improvements in the results indicate the superiority of the former.**

I. Introduction

Multicarrier modulation (MCM) techniques have been preferred over single carrier methods in the majority of the current wireless communication standards. This is indeed due to the several advantages they offer, among which, the ease of equalization in frequency selective environment is prominent. Orthogonal frequency division multiplexing (OFDM), as the most established form of MCM, has been largely studied and adopted in many wireless and wireline standards [1], [2]. Nevertheless, in recent years, a variant of OFDM based on offset quadrature amplitude modulation (OFDM/OQAM) has attracted much research attention. This is due to its several benefits over conventional OFDM, including higher spectral efficiency and reduced sensitivity to timing and frequency mismatch [3]. However, for successful application of OFDM/OQAM in practical systems in the future, accurate carrier frequency and timing synchronization along with channel estimation (for the purpose of equalization) remain imperative. Since in practical scenarios, the required training symbol overhead is usually tolerated, our focus here is on pilot-based synchronization and channel estimation.

Despite the relative abundance of literature for estimation of carrier frequency offset (CFO), sampling time offset (STO) or channel impulse response (CIR) in single-user OFDDM/OQAM, the multiuser case has received very limited attention. This is in spite of the fact that estimation of the aforementioned parameters in a multiuser scenario seems crucial, assuming that, similar to the current standards, multiple access on a shared transmultiplexer (e.g. in the uplink) will continue to exist in the future generations of communication systems. One of the few works on parameter estimation in multiuser OFDM/OQAM is presented in [4], proposing an ML symbol timing estimator derived by using two training symbols per burst transmission. The authors investigate the effect of different types of subcarrier allocation to different users, i.e. blockwise and interleaved allocations. In [5], they incorporate the CFO estimation to their timing estimator. In [6], the authors propose estimating the CFO using the correlation of the received pilot symbols in frequency domain (i.e. based on the filter bank outputs) and include STO estimation based on maximizing the energy across subcarriers for the desired user.

In [7], we developed a joint pilot-based ML estimator of the CFO, STO and CIR in single-user OFDM/OQAM systems. Herein, we extend our estimator to multiuser scenarios. We also deploy the real orthogonality principle of OFDM/OQAM systems. As such, the current work proposes an improved pilot-based joint ML estimation method of the CFO, STO and CIR in multiuser OFDM/OQAM systems built upon the assumption of Gaussian noise and independent input symbols. In addition, the problem is formulated by splitting the interference to a received pilot to contributions from subband noise, surrounding data-bearing symbols and multiuser interference. By investigating the statistical properties of the aforementioned interference terms, the ML estimator is obtained. Simulation results for different subcarrier allocation schemes and burst types show the superior performance of the proposed method as compared to a highly cited previous work of the same focus as benchmark.

In Section II, first the OFDM/OQAM system model, as adopted in this work, is presented. Next, this generic system model is modified to represent a multiuser scenario where multiple users share one transmultiplexer. In Section III, the multiuser estimator is derived, based on the aforementioned assumptions, by observing and analyzing the statistical properties of the interference terms. Simulation results are depicted and discussed in Section IV comparing the proposed method. Section V concludes this paper.

II. System Model

In this section, we first review the generic OFDM/OQAM system model as implemented in this work. Next, we present the essential modifications to the system model for a multiuser scenario where different users share one OFDM/OQAM transmultiplexer.

This research was funded by the Natural Sciences and Engineering Research Council (NSERC) of Canada.

978-1-5386-4784-2/18/$31.00 ©2018 IEEE

A. Single-user OFDM/OQAM System Model

The OFDM/OQAM system model, adopted in this work, makes use of a specific filter bank structure where the up-sampling and downsampling factor equals half the number of subcarriers, denoted by M (see [8] Fig. 1). At each input symbol time, with symbol duration T_s, a vector of discrete input symbols is loaded on the M available subcarriers. The latter are separated in frequency by $F_s = 1/T_s$, so that the system occupies a total bandwidth of $W = MF_s$.

On the transmitter side, let $x_{k,n} \in \mathcal{A}$ denote the complex valued input symbols, where $k \in \{0, 1, \ldots, M-1\}$ is the subcarrier index, $n \in \mathbb{Z}$ is the symbol time index, and $\mathcal{A}$ is the digital constellation from which the symbols are drawn. In the first stage of pre-processing, each $x_{k,n}$ is converted to a pair of real symbols, $d_{k,n}$, according to equations (2)-(3) in [8]. This complex-to-real (C2R) operation doubles the sampling rate of the subcarrier signals. The second stage of pre-processing involves multiplication of the real OQAM symbols, $d_{k,n}$, by the sequence $\theta_{k,n} = e^{j\frac{\pi}{2}(k+n)}$, which results in complex symbols

$$s_{k,n} = d_{k,n}\theta_{k,n} = d_{k,n}e^{j\frac{\pi}{2}(k+n)}\,. \tag{1}$$

It is notable that the OQAM symbol duration is $T_s/2$, i.e. one half of the input symbol duration. Next, in the synthesis filter bank (SFB), the input subcarrier signals $s_{k,n}$ are first upsampled by $M/2$, and then passed through synthesis filters with finite impulse responses (FIR) $f_k[m]$ of length L_p and corresponding system functions $F_k(z) = \sum_{m=0}^{L_p-1} f_k[m]z^{-m}$. Finally, the individual filter outputs are added together to form the baseband output $y[m]$ as follows,

$$y[m] = \sum_{k=0}^{M-1}\sum_{n\in\mathbb{Z}} s_{k,n}\, f_k\Big[m - \frac{nM}{2}\Big] \tag{2}$$

On the receiver side, let $\bar{y}[m]$ denote the received baseband signal after transmission through the noisy channel. In the analysis filter bank (AFB), signal $\bar{y}[m]$ is passed through the analysis filters with FIR $g_k[m]$ of length L_p and corresponding system functions[1] $G_k(z) = \sum_{m=-L_p+1}^{0} g_k[m]z^{-m}$, whose outputs are downsampled by $M/2$ afterwards. The resulting symbols at the output of the AFB can be represented as

$$\bar{s}_{k,n} = \sum_{m=-\infty}^{\infty} \bar{y}[m]g_k\Big[\frac{nM}{2} - m\Big] \tag{3}$$

where the range of summation over m is determined by the finite support of the subband FIR filters. The symbols $\bar{s}_{k,n}$ then pass through the first post-processing stage, which involves multiplication by the sequence $\theta^*_{k,n}$ followed by taking the real part, i.e.,

$$\bar{d}_{k,n} = \Re[\bar{s}_{k,n}\,\theta^*_{k,n}] = \Re[\bar{s}_{k,n}\,e^{-j\frac{\pi}{2}(k+n)}] \tag{4}$$

The second post-processing stage is the real-to-complex (R2C) conversion, where two consecutive real valued symbols are combined into a complex one as in equation (7) in [8]. We consider a complex-valued, uniform modulated filter bank, where the subchannel filters are all generated from a common low-pass prototype filter, $p[m]$, by means of exponential modulation as follows,

$$f_k[m] = p[m]e^{j\frac{2\pi km}{M}}\,,\;\; g_k[m] = f^*_k[-m]\,, \tag{5}$$

[1]For convenience in our analysis, $G_k(z)$ is assumed non-causal; although, in practice, causality can be restored simply by introducing an appropriate delay in the receiver.

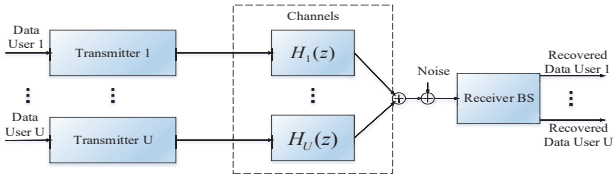

Fig. 1: Uplink transmissions in multiuser systems

where $k \in \{0, 1, ..., M-1\}$. The prototype filter used in this work, known as PHYDYAS filter, is a near perfect reconstruction (NPR), real-valued linear phase (symmetric) FIR low-pass filter with length L_p and support region $m \in \{0, 1, \ldots, L_p - 1\}$. It is derived by using the frequency sampling technique, as in [8], with overlap factor $K = 4$. Since the prototype filter is linear-phase, the overall processing delay of the complete OFDM/OQAM transceiver system will be L_pT_s/M. By using the paraconjugates of the synthesis filters as the analysis filters in the receiver, as specified in (5), the orthogonality condition of the transceiver system can be expressed as

$$\Re\Big\{\theta^*_{k,n}\theta_{k',n'}\sum_{m=-\infty}^{\infty} f^*_k[m - \frac{nM}{2}]\; f_{k'}[m - \frac{n'M}{2}]\Big\} \approx \delta_{kk'}\delta_{nn'} \tag{6}$$

where $\delta_{kk'}$ denotes the Kronecker delta function[2].

B. System Model Modification for a Multiuser Scenario

As depicted in Fig. 1, we consider a multiuser scenario where, in the uplink of a multiple access system, users 1 to U transmit their pilot and data symbols over the channel to the same base station. We assume the users are not necessarily experiencing identical CFO, STO and CIR and that the aforementioned parameters for different users are decoupled from one another. To employ the proposed OFDM/OQAM system in a multiuser scenario, as depicted in Fig. 2, the necessary modification is to consider the relevant subcarriers or samples associated with the desired user. Specifically, we denote by $\mathcal{S}_u$ the set of subcarrier indexes allocated to the uth user. The cardinal of this set $|\mathcal{S}_u|$ represents the total number of subcarriers allocated to this user. Hence, the transmitter output signal of associated with this user at discrete time mT_s/M, is given by

$$y_u[m] = \sum_{k\in\mathcal{S}_u}\sum_{n} s^u_{k,n} f^u_k[m - \frac{nM}{2}] \tag{7}$$

where the subscripts and superscripts u indicate that the quantity (e.g. the symbol or the filter) is associated with the uth user.

Assuming that during a time interval equal to the processing delay of the transceiver system (i.e. L_pT_s/M) the transmission channel of the uth user can be modeled as a linear time-invariant system with FIR $h_u[l]$ of length Q and corresponding transfer function $H_u(z) = \sum_{l=0}^{Q-1} h_u[l]z^{-l}$, in

[2]In [7], to simplify the derivation of the joint ML estimator, complex orthogonality of the analysis/synthesis filters is assumed. Since in practical OFDM/OQAM systems, these filters only need satisfy a weaker real orthogonality condition, the resulting joint estimator is sub-optimal.

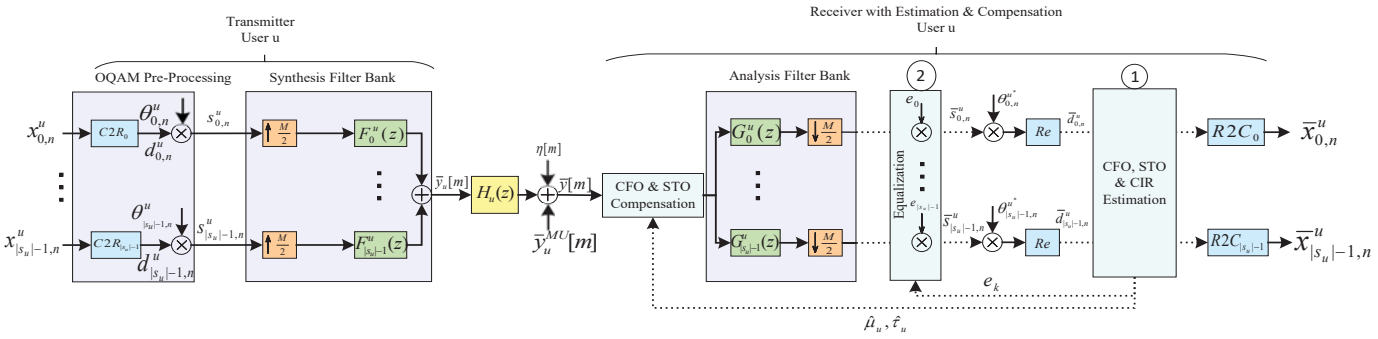

Fig. 2: Transceiver chain of the uth user in a multiuser OFDM/OQAM system with CFO, STO and channel estimation and compensation

the presence of CFO and STO the received signal from the uth user can be modeled as

$$\bar{y}_u[m] = e^{-j2\pi \frac{\mu_u}{M} m} \sum_{l=0}^{Q-1} h_u[m] y_u[m - l - \tau_u] \tag{8}$$

where μ_u is the normalized CFO of user u with respect to the subcarrier spacing F_s whereas τ_u is their normalized STO with respect to the OQAM symbol duration $T_s/2$.

The received baseband signal $\bar{y}[m]$ can be expressed as [9],

$$\bar{y}[m] = \bar{y}_u[m] + \bar{y}_u^{MU}[m] + \eta[m] \tag{9}$$

where $\bar{y}_u[m]$ represents the contribution of the user of interest u to the received signal, $\bar{y}_u^{MU}[m]$ represents the contribution from other users, and $\eta[m]$ denotes the additive white Gaussian noise (AWGN) with zero mean and variance $E\{|\eta[m]|^2\} = \frac{\sigma_\eta^2}{2}$ (where $E\{.\}$ denotes statistical expectation), which is assumed statistically independent from the input data. The contribution from other users can be written as the summation of the received signals associated with other users as shown in the following equation,

$$\bar{y}_u^{MU}[m] = \sum_{\substack{v=1 \\ v \neq u}}^{U} \bar{y}_v[m] \tag{10}$$

where U and v denote the number of users and the user index respectively.

III. Multiuser Estimation

A. Received Symbols and Interference Terms

The received signal $\bar{y}[m]$ is passed through the analysis filter bank (AFB) and downsampled by $M/2$. Hence, the reconstructed signal for the kth subcarrier of the uth user can be written as

$$\bar{d}_{k,n}^u = \Re\{\theta_{k,n}^{u^*} \bar{s}_{k,n}^u\} = \Re\Big\{\theta_{k,n}^{u^*} \sum_m \bar{y}[m] g_k^u[\frac{nM}{2} - m]\Big\}. \tag{11}$$

For clarity in the presentation, we define $d_{k,n}^u \equiv d_{k,n}^d$; that is, the transmitted data symbols (i.e., non-pilot) corresponding to the desired user u are denoted as $d_{k,n}^d$ where $k \in \mathcal{S}_u$. As well, we note that in $d_{k,n}^d$, we have $(k,n) \notin \mathcal{P}_u$, where $\mathcal{P}_u$ represents the set containing all time-frequency locations of the pilots associated with user u. These symbols, unknown to the receiver, are modeled as independent and identically distributed (i.i.d.) random variables with zero-mean and variance $\frac{1}{2}\sigma_x^2$. Similarly, the corresponding received symbols are denoted as $\bar{d}_{k,n}^d$.

For the received pilot at subcarrier k and time index n, associated with the uth user, altering $\bar{d}_{k,n}^u$ to $\bar{d}_{k,n}^p$, we have [3]

$$\bar{d}_{k,n}^p = \zeta_{k,n}^p + \zeta_{k,n}^d + \psi_{k,n}^{MU} + \eta_{k,n}\,, \tag{12}$$

where $\zeta_{k,n}^p$ and $\zeta_{k,n}^d$ respectively denote the contributions from surrounding pilots and data, $\psi_{k,n}^{MU}$ stands for the 'multiple access interference' (MAI), and $\eta_{k,n}$ represents the additive noise (i.e. the contribution from $\eta[m]$) passed through the AFB and the first post-processing stage, as given by

$$\eta_{k,n} = \Re\Big\{\theta_{k,n}^{u^*} \sum_{m=-\infty}^{\infty} \eta[m]\; g_k^u[\frac{nM}{2} - m]\Big\}. \tag{13}$$

From (1), (5), (7)–(9), (11) and (12) the pilot contribution can be expressed as

$$\zeta_{k,n}^p = \Re\Big\{\sum_{l=0}^{Q-1} h_u[l] \bar{\lambda}_{k,n}(l, \mu_u, \tau_u)\Big\} \tag{14}$$

where the term $\bar{\lambda}_{k,n}(l, \mu_u, \tau_u)$ represents the contribution from all the pilot symbols to the received pilot symbol $\bar{d}_{k,n}^p$, affected by the lth channel coefficient as given by

$$\bar{\lambda}_{k,n}(l, \mu_u, \tau_u) = \sum_{(k',n') \in \mathcal{P}_u} d_{k',n'}^p \gamma_{k,n}^{k',n'}(l, \mu_u, \tau_u) \tag{15}$$

$$\gamma_{k,n}^{k',n'}(l, \mu_u, \tau_u) = \theta_{k,n}^{u^*} \theta_{k',n'}^u \sum_{m=-\infty}^{\infty} f_{k'}^u\big[m - l - \tau_u - \frac{n'M}{2}\big] f_k^{u^*}\big[m - \frac{nM}{2}\big] e^{-j2\pi m \frac{\mu_u}{M}} \tag{16}$$

The complex factor $\gamma_{k,n}^{k',n'}(l, \mu_u, \tau_u)$, called the 'ambiguity function', characterizes the interference level of the n'th input sample from the k'th subband (belonging to user u) on the nth output sample of the kth subband (belonging to the same user), in the presence of CFO with magnitude μ_u and STO, τ_u, affected by the lth coefficient of the channel between this user and the base station.

[3] For notational convenience, hereafter, we shall drop the superscripts and subscripts u for all the quantities except for the subcarrier filters $f_k^u[.]$ and $g_k^u[.]$, the sequences $\theta_{k,n}^u$ and $\theta_{k,n}^{u^*}$, and the parameters under estimation, τ_u, μ_u and h_u.

Similarly, from (1), (5), (7)–(9), (11) and (12) the data contribution from the same user, which in the present context can be interpreted as "data interference", can be expressed as

$$\zeta_{k,n}^{d} = \sum_{(k',n')\notin\mathcal{P}_u} d_{k',n'}^{d}\Re\Big\{\sum_{l=0}^{Q-1} h_u[l]\gamma_{k,n}^{k',n'}(l,\mu_u,\tau_u)\Big\} \quad (17)$$

Finally, from (11) and (12), the total contribution to the received pilot of user u at time-frequency location (k,n), $\bar{d}_{k,n}^{p}$, from other users' transmitted symbols (pilot and data), is given by

$$\psi_{k,n}^{MU} = \Re\Big\{\theta_{k,n}^{u^*}\sum_{m}\bar{y}^{MU}[m]g_k^u[\frac{nM}{2}-m]\Big\}. \quad (18)$$

Based on the foregoing assumption on additive noise in (9) and the orthogonality condition for the subcarrier filters in (6) we can show that the subcarrier noise symbols $\eta_{k,n}$ are normally distributed with zero mean and covariance of

$$E\{\eta_{k,n}\eta_{k',n'}\} = \frac{\sigma_\eta^2}{2}\delta_{kk'}\delta_{nn'}\,. \quad (19)$$

In addition, if we model the input signals from the interfering users, i.e. $x_{k,n}^{v}$ for all $v\neq u$ and $k\in\mathcal{S}_v$, as independent zero-mean white data sequences with variance σ_x^2, it follows from (1), (7)–(10) and (18) that the multiuser interference term $\psi_{k,n}^{MU}$ is the sum of a large number of independent random contributions; thus, based on the central limit theorem [10], it can be approximated as a normally distributed random variable with zero mean. Hence, we assume that this term can be modeled as a white noise sequence, i.e. with covariance

$$E\{\psi_{k,n}^{MU}\psi_{k',n'}^{MU}\} \approx \sigma_\psi^2\,\delta_{kk'}\delta_{nn'} \quad (20)$$

where σ_ψ^2 is the corresponding variance. Numerical simulations have been performed to verify the validity of this assumption. In practice, the variance σ_ψ^2 can be obtained based on the measurements of multiuser interference power.

In view of the assumptions made above on $d_{k,n}^{d}$, we note that the expression (17) involves the weighted sum of a large number of statistically independent, zero-mean terms $d_{k',n'}^{d}$. Hence, invoking the central limit theorem, we shall assume that $\zeta_{k,n}^{d}$ in (17) can be modeled as a zero-mean (real-valued) Gaussian random process. In addition, under mild assumptions usually satisfied in practice, it can be shown that the random variables $\zeta_{k,n}^{d}$ (for different pairs (k,n)) are nearly uncorrelated. Specifically, we can show that

$$E\left\{\zeta_{k,n}^{d}\zeta_{k',n'}^{d}\right\} \approx \frac{\sigma_{\zeta^d}^2}{2}\,\delta_{kk'}\delta_{nn'}\,, \quad (21)$$

where

$$\sigma_{\zeta^d}^2 = \frac{\sigma_x^2}{2}\sum_{(k',n')\notin\mathcal{P}_u}(\Re\{\sum_{l} h_u[l]\gamma_{k,n}^{k',n'}(l,\mu_u,\tau_u)\})^2\,. \quad (22)$$

From (12), (19)–(21) by introducing $v_{k,n} = \zeta_{k,n}^{d} + \psi_{k,n}^{MU} + \eta_{k,n}$ and assuming that the data and the additive noise are statistically independent, it follows that the terms $v_{k,n}$ are independent Gaussian random variables with variance $\sigma_v^2 = \sigma_{\zeta^d}^2 + \sigma_\psi^2 + \frac{\sigma_\eta^2}{2}$. Finally, by substituting $v_{k,n}$ in (12) we have

$$\bar{d}_{k,n}^{p} = \zeta_{k,n}^{p} + v_{k,n}\,, \quad (23)$$

which provides a convenient basis for the derivation of the coveted ML estimator.

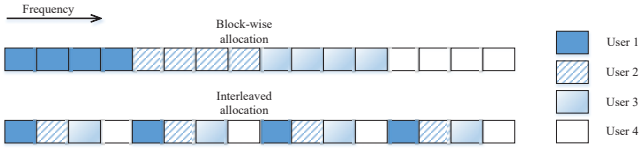

Fig. 3: Allocation schemes with $U=4$ users over $M=16$ subcarriers

B. Estimator Derivation

Focusing on the pilot contribution in (14), we have

$$\zeta_{k,n}^{p} = \Re\Big\{\sum_{l=0}^{Q-1} h_u[l]\bar{\lambda}_{k,n}(l,\mu_u,\tau_u)\Big\} \quad (24)$$

$$= \sum_{l=0}^{Q-1}\left(h_u^R[l]\bar{\lambda}_{k,n}^R(l,\mu_u,\tau_u) - h_u^I[l]\bar{\lambda}_{k,n}^I(l,\mu_u,\tau_u)\right), \quad (25)$$

where the superscripts R and I are used to identify the real and imaginary parts of the underlying quantity. Hence, by letting

$$\boldsymbol{\lambda}_{k,n}^R(\mu_u,\tau_u) = [\bar{\lambda}_{k,n}^R(0,\mu_u,\tau_u),\ldots,\bar{\lambda}_{k,n}^R(Q-1,\mu_u,\tau_u)]\,,$$
$$\boldsymbol{\lambda}_{k,n}^I(\mu_u,\tau_u) = [\bar{\lambda}_{k,n}^I(0,\mu_u,\tau_u),\ldots,\bar{\lambda}_{k,n}^I(Q-1,\mu_u,\tau_u)]\,,$$
$$\mathbf{h}_u^R = [h_u^R[0],\ldots,h_u^R[Q-1]],\quad \mathbf{h}_u^I = [h_u^I[0],\ldots,h_u^I[Q-1]]\,,$$

we can obtain the relationship between the received symbol and the channel taps as

$$\zeta_{k,n}^{p} = \Big[\boldsymbol{\lambda}_{k,n}^R(\mu_u,\tau_u)\ \ \boldsymbol{\lambda}_{k,n}^I(\mu_u,\tau_u)\Big]_{1\times 2Q}\begin{bmatrix}\mathbf{h}_u^R\\ -\mathbf{h}_u^I\end{bmatrix}_{2Q\times 1}. \quad (26)$$

By stacking $\bar{d}_{k,n}^{p}$, $\boldsymbol{\lambda}_{k,n}^R(\mu_u,\tau_u)$ and $\boldsymbol{\lambda}_{k,n}^I(\mu_u,\tau_u)$, and $v_{k,n}$ over the time index n and then over the frequency index k, we arrive at the following matrix-vector equation

$$\Big[\bar{\boldsymbol{D}}^{\boldsymbol{p}}\Big]_{N_p\times 1} = \underbrace{\Big[\boldsymbol{\Lambda}^R(\mu_u,\tau_u)\ \ \boldsymbol{\Lambda}^I(\mu_u,\tau_u)\Big]}_{\boldsymbol{\Lambda}'(\mu_u,\tau_u)}\underbrace{\begin{bmatrix}\mathbf{h}_u^R\\ -\mathbf{h}_u^I\end{bmatrix}}_{\mathbf{h}'}$$
$$N_p\times 2Q \qquad 2Q\times 1$$
$$+\Big[\boldsymbol{V}\Big]_{N_p\times 1}. \quad (27)$$

where N_p represents the number of pilots. As a result of the AWGN assumption and the ensuing assumptions on the noise and interference terms $\eta_{k,n}$, $\psi_{k,n}^{MU}$ and $\zeta_{k,n}^{d}$, $\boldsymbol{V}$ is a real Gaussian random vector with zero mean and a nearly diagonal covariance matrix $\boldsymbol{C_V} = \mathrm{E}[\boldsymbol{V}\boldsymbol{V}^T] \approx \sigma_v^2\boldsymbol{I}$. Similarly, for given values of μ_u, τ_u and $\mathbf{h}$, the observation $\bar{\boldsymbol{D}}^{\boldsymbol{p}}$ is also a Gaussian random vector with mean $\boldsymbol{\Lambda}'(\mu_u,\tau_u)\mathbf{h}'$ and covariance $\boldsymbol{C}_{\bar{\boldsymbol{D}}^{\boldsymbol{p}}} \approx \sigma_v^2\boldsymbol{I}$. Hence, the probability density function (PDF) of $\bar{\boldsymbol{D}}^{\boldsymbol{p}}$ can be presented as

$$f(\bar{\boldsymbol{D}}^{\boldsymbol{p}};\mu_u,\tau_u,\mathbf{h}') = \frac{1}{\sqrt{(2\pi)^{N_p}\det(\boldsymbol{C}_{\bar{\boldsymbol{D}}^{\boldsymbol{p}}})}} \quad (28)$$
$$\exp\Big[-\frac{1}{2}(\bar{\boldsymbol{D}}^{\boldsymbol{p}}-\boldsymbol{\Lambda}'(\mu_u,\tau_u)\mathbf{h}')^T\boldsymbol{C}_{\bar{\boldsymbol{D}}^{\boldsymbol{p}}}^{-1}$$
$$(\bar{\boldsymbol{D}}^{\boldsymbol{p}}-\boldsymbol{\Lambda}'(\mu_u,\tau_u)\mathbf{h}')\Big]$$

Thus, the log-likelihood function (LLF) is written, up to a constant, as

$$\mathcal{L}(\bar{\boldsymbol{D}}^{\boldsymbol{p}};\mu_u,\tau_u,\mathbf{h}') = \log(f(\bar{\boldsymbol{D}}^{\boldsymbol{p}};\mu_u,\tau_u,\mathbf{h}')) \quad (29)$$
$$= -\frac{1}{2\sigma_v^2}[\bar{\boldsymbol{D}}^{\boldsymbol{p}} - \boldsymbol{\Lambda}'(\mu_u,\tau_u)\mathbf{h}']^T [\bar{\boldsymbol{D}}^{\boldsymbol{p}} - \boldsymbol{\Lambda}'(\mu_u,\tau_u)\mathbf{h}']$$

The joint ML estimators of the CFO, CIR and STO can be obtained by maximizing the derived LLF with respect to the parameters μ_u, τ_u and $\mathbf{h}'$. Let the search parameters for CFO and STO be denoted by $\tilde{\mu}_u$ and $\tilde{\tau}_u$. By fixing $\tilde{\mu}_u$ and $\tilde{\tau}_u$ and varying $\mathbf{h}'$ in $\mathbb{C}^{2Q}$, the LLF achieves its maximum at

$$\tilde{\mathbf{h}'}(\mu_u,\tau_u) = \boldsymbol{\Lambda}'(\mu_u,\tau_u)^\dagger \bar{\boldsymbol{D}}^{\boldsymbol{p}} \quad (30)$$

where $\boldsymbol{\Lambda}'(\mu_u,\tau_u)^\dagger = (\boldsymbol{\Lambda}'(\mu_u,\tau_u)^T\boldsymbol{\Lambda}'(\mu_u,\tau_u))^{-1}\boldsymbol{\Lambda}'(\mu_u,\tau_u)^T$ is the pseudo-inverse of $\boldsymbol{\Lambda}'(\mu_u,\tau_u)$. By substituting the resulting channel guess of (30) into the LLF we can obtain the CFO and STO estimates using a two-dimensional search according to

$$(\hat{\mu}_u,\hat{\tau}_u) = \underset{(\tilde{\mu}_u,\tilde{\tau}_u)}{\arg\max}\, \mathcal{L}(\bar{\boldsymbol{D}}^{\boldsymbol{p}};\tilde{\mu}_u,\tilde{\tau}_u,\tilde{\mathbf{h}'}) \quad (31)$$

The ML estimate of the CIR can be obtained by substituting the estimates $(\hat{\mu}_u,\hat{\tau}_u)$, resulting in[4].

$$\hat{\mathbf{h}'} = \tilde{\mathbf{h}'}(\hat{\mu}_u,\hat{\tau}_u) = \boldsymbol{\Lambda}'(\hat{\mu}_u,\hat{\tau}_u)^\dagger \bar{\boldsymbol{D}}^{\boldsymbol{p}} \quad (32)$$

IV. Simulation Setup and Results

To evaluate the performance of the proposed estimator in a multiuser scenario, we compare the estimation results with one of the few works on multiuser estimation for OFDM/OQAM systems, i.e. [5]. For both methods, an OFDM/OQAM transceiver with 1024 subcarriers have been implemented where 256 subcarriers are assigned to each user in two different subcarrier allocation schemes with no dropped subcarrier, i.e. blockwise allocation and interleaved allocation. This is depicted in Fig. 3. Furthermore, in the evaluation of the proposed estimator, in addition to the preamble-data burst transmission mode, a scattered pilot-data mode is also simulated where both burst modes share an identical data rate. Each user experiences an independent CFO, STO and CIR. In each preamble-data burst, a preamble consisting of 4 input symbols, followed by 24 data symbols is used in both methods. root-mean-squared error (RMSE) results of CFO, STO and CIR estimation have been averaged over all the users. To this goal, while the SNR-per-bit value of the desired user varied from 0 to 20 dB, the other three users experienced a fixed value of 20 dB. To obtain the RMSE error of CFO estimation, the STO of all users is fixed at 2.5% of T_s while they experience different CFOs randomly chosen from the interval $[-F_s/4 \;\; F_s/4]$. As for the RMSE error of STO estimation, the CFO of all users is fixed at 5% of subcarrier spacing while they experience different STO randomly chosen in the interval $[-T_s/4 \;\; T_s/4]$. It is assumed that the users experience independent frequency selective wireless channel multipath channels, all realized based on the ITU-Vehicular A [11] with $Q = 8$ randomly generated coefficients $h_u[l]$ with Rayleigh distribution where the 5th and the 7th tap are set to zero and the other taps follow the power profile $[0, -1, -9, -10, -15, -20]$ in dB. The channel is constant during the transmission of a burst but changes over different transmissions.

[4]To reduce the computational complexity of the algorithm, two simplifications are added to the computation of $\bar{\lambda}_{k,n}(l,\mu_u,\tau_u)$ in (27); the first based on the phase relationship between the filters at different subchannels and the second based on neglecting the subcarriers beyond ± 2. In addition, to make the two-dimensional search for CFO and STO more practical, only the first 3 channel taps, i.e. those with greatest contributions, are considered in the computation of the RHS of (24).

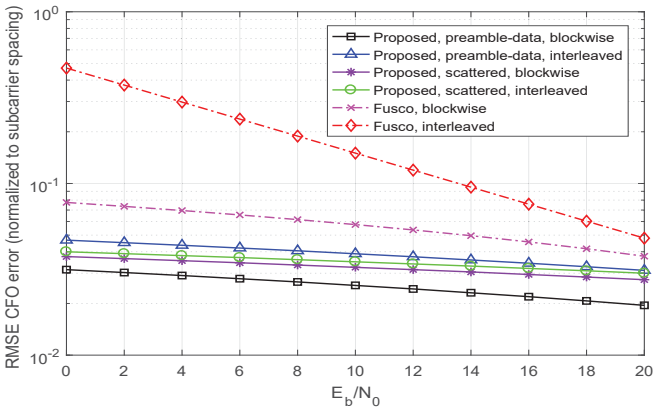

Fig. 4: Comparative multiuser RMSE of CFO estimation versus input E_b/N_0 in presence of STO and Rayleigh channel

In coded BER simulation results, both the CFO and STO of all the users are randomly chosen in the intervals mentioned above. These are then estimated and compensated for all the users. The channel is, however, considered known and perfectly equalized at the receiver since the benchmark method does not include channel estimation. To obtain BER that are more representative of a practical digital communications system, a punctured convolutional channel coding scheme is applied to the information sequence with the overall rate of $2/3$ by using constraint lengths vector $[5 \;\; 4]$ and vector of function generators $[23 \;\; 35 \;\; 0; \;\; 0 \;\; 5 \;\; 13]$. The RMSE estimation results of CFO and STO, in [5], are obtained in the absence of the other impairment whereas, in this work, the other impairment is always present. Another modification in our implementation of [5] is the aforementioned 8-tap multipath channel used in our work as opposed to the 6-tap channel therein. The third adjustment is the use of a 4-symbol preamble rather than a 1-symbol preamble. The other parameters, including the prototype filter used are adopted as identical to the paper.

Fig. 4 depicts the multiuser CFO estimation results of the proposed method as compared to [5]. In this figure, the RMSE estimation errors of the two methods with respect to E_b/N_0 are compared for two different pilot distributions schemes, in the proposed method, and two subcarrier allocation schemes in both methods. As can be seen, the proposed method outperforms the benchmark in all the configurations. More specifically, the lowest RMSE error belongs to the proposed method in preamble-data distribution when the subcarriers are blockwise allocated to the four users. The figure suggests that the scattered-blockwise configuration slightly surpasses the scattered-interleaved configuration since the interleaved subcarrier allocation enhances the multiuser interference. However, the scattered-interleaved configuration renders slightly less error as compared to the preamble-interleaved configuration. In an interleaved allocation, this can be viewed due to the higher mutual interference of pilots of different users in the preamble-data type of burst as compared to the scattered

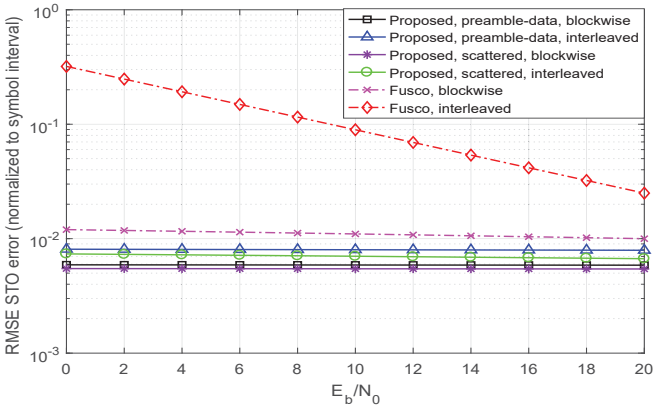

Fig. 5: Comparative multiuser RMSE of STO estimation versus input E_b/N_0 in presence of CFO and Rayleigh channel

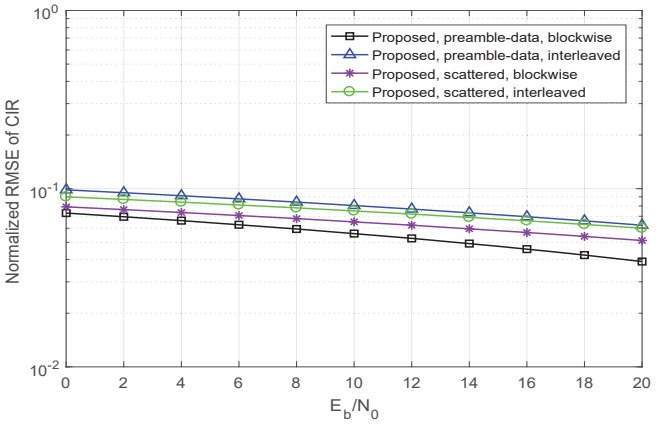

Fig. 6: Comparative multiuser RMSE of CIR estimation versus input E_b/N_0 in presence of CFO and STO

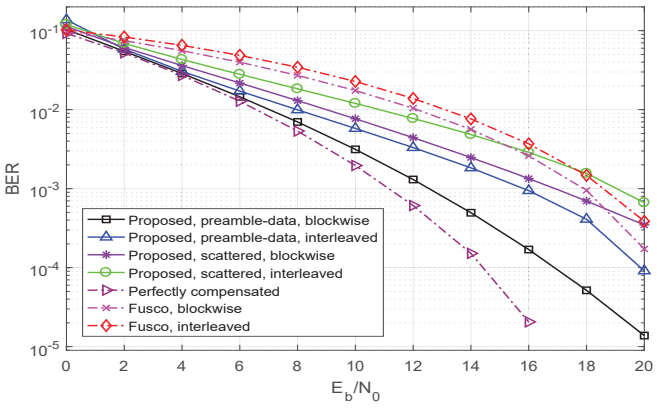

Fig. 7: Comparative BER versus input E_b/N_0 in presence of CFO, STO and Rayleigh channel

burst.

In Fig. 5, the multiuser RMSE error of STO estimation is illustrated. The figure shows that, except for the method in [5] with the interleaved allocation, the other implementations do not significantly vary with E_b/N_0. In addition, in all configurations, the proposed method offers lower STO estimation error than those of [5]. Our simulation results show that, in Fig. 4 and 5, the RMSE will plateau to an error floor above that of the proposed methods, which is expected given the assumption made on the noise and data interference terms.

Fig. 6 depicts the simulation results of CIR estimation versus input E_b/N_0 in presence of CFO and STO for the proposed method in different configurations. As can be seen, the same trend is maintained between different configurations. No channel estimation is reported in the existing literature for the multiuser case.

Finally, Fig. 7 illustrates the multiuser coded BER simulation result of the two methods versus input E_b/N_0 in the presence of the CFO and STO estimation and compensation as well as a perfectly equalized multipath fading channel. In this figure, similarly, the superior performance of the proposed method is observable as compared to that of [5].

V. Conclusion

A new general pilot-based ML joint estimation method for multiuser OFDM/OQAM systems has been developed and evaluated. The CFO, STO and CIR effects have been jointly estimated. Performance evaluation has been carried out through comparison with a highly-cited method among the few research papers of the same focus. Two subcarrier allocation schemes, namely blockwise and interleaved, and two different transmission modes, i.e. preamble-data and scattered pilots have been considered. The results have shown the significant improvement that the proposed method offers with both subcarrier allocation schemes. As it was observed, the proposed estimator, especially when used in a preamble-data setup with blockwise allocation, can robustly estimate the CFO, STO and CIR. In addition, the BER and RMSE curves indicate superiority of the blockwise subcarrier allocation compared to the interleaved one.

References

[1] L. Hanzo, Y. Akhtman, L. Wang, and M. Jiang, *OFDM for Wireless Multimedia Communications*, John Wiley, Hoboken, NJ, USA, 2011.

[2] P. Golden, H. Dedieu, and K.S. Jacobsen, *Fundamentals of DSL Technology*, CRC Press, 2005.

[3] B. Farhang-Boroujeny, "OFDM versus filter bank multicarrier," *IEEE Signal Process. Mag.*, vol. 28, pp. 92–112, May, 2011.

[4] T. Fusco, A. Petrella, and M. Tanda, "Data-aided symbol timing estimation for multiple-access OFDM/OQAM systems," in *Proc. IEEE Int. Conf. Communications (ICC)*, June 2009, pp. 1–5.

[5] T. Fusco, A. Petrella, and M. Tanda, "Joint symbol timing and CFO estimation in multiuser OFDM/OQAM systems," in *SPAWC*, June 2009, pp. 613–617.

[6] H. Saeedi-Sourck and S. Sadri, "Frequency-domain carrier frequency and symbol timing offsets estimation for offset QAM filter bank multicarrier systems in uplink of multiple access networks," in *Wireless Personal Commun.*, May 2013, vol. 70, pp. 601–615.

[7] A. Baghaki and B. Champagne, "Joint carrier frequency offset, sampling time offset and channel estimation for OFDM-OQAM systems," in *VTC*, Boston, MA, USA, Sep. 2015.

[8] A. Viholainen et al., "Prototype filter design for filter bank based multicarrier transmission," in *EUSIPCO*, Glasgow, Scotland, Aug. 2009, vol. 17, pp. 1359–1363.

[9] S. Rahimi and B. Champagne, "Joint synchronization and equalization in the uplink of multi-user OPRFB transceivers," in *GLOBECOM*, 2014, pp. 3407–3412.

[10] J.A. Rice, *Mathematical Statistics and Data Analysis*, Number p. 3 in Advanced series. Cengage Learning, 2007.

[11] "ITU-R M.Guidelines for evaluation of radio transmission technologies for IMT-2000 1225," 1997.